Citation: Lijun Han, Rui Wang, Fuyang Liu. Numerical simulation analysis of FSPR joint forming for steel/Al alloy hybrid body-in-white. *Journal of Harbin Institute of Technology (New Series)*. DOI: 10.11916/j.issn.1005-9113.24013

Numerical Simulation Analysis of FSPR Joint Forming for Steel/Al Alloy Hybrid Body-in-White

Lijun Han[1,*], *Rui Wang*[2] *and Fuyang Liu*[1]

(*1. FAW-Volkswagen Automotive Company, Changchun 130011, China;*
2. College of Materials Science and Engineering, Jilin University, Changchun 130025, China)

Abstract: The development and application of large Die-Casting Al Alloy (DCAA) parts and Thermo-Formed Steel Sheets (TFSS) in Body-In-White (BIW) have created higher demands for the joining technology of high-strength steel/Al dissimilar materials. As an emerging technology, Flush Self-Piercing Riveting (FSPR) is still in the experimental phase and undergoing small batch equipment verification. This paper focuses on the joining methods for DCAA and TFSS in BIW, investigating the joining mechanisms, technical features, and forming principles of FSPR for steel/Al dissimilar materials with two-layer or three-layer plate combinations. Considering the TL4225/C611/CR5 sheet combination as a subject, the forming mechanism of high-quality joints was studied, and a physical and mathematical model was established to depict the relationship between the filling amount of the arc-gap and die dimensions, as well as the extrusion amount. This model effectively illustrates the relationship between the filling amount of the flowing metal in the arc-gap and critical parameters, such as die dimensions and feeding amounts. By simplifying the process of selecting joining parameters, it significantly reduces both the time and experimental workload associated with parameter selection. This provides a technical foundation for the application of DAAA and TFSS parts in BIW, enabling the rapid choice of appropriate joining parameters to meet the requirements for obtaining high-quality joints. The model can be effectively utilized to investigate the relationships between key parameters, including arc-gap radius, plate thickness, rivet arc radius, nail head radius, groove width, and feeding amount, while keeping other parameters constant. This approach provides a theoretical foundation for the design of Friction Stir Processing (FSPR) joints and aids in the selection of optimal parameters.

Keywords: FSPR; joining; DCAA; TFSS; two or three-layer plate
CLC number: TG444 **Document code**: A **Article ID**: 1005-9113(2024)00-0000-08

0 Introduction

Light weighting is an inevitable trend in the development of the car body, and a notable feature of future BIW is the combination of TFSS and large DCAA, which can meet the requirements of body safety, light weighting and energy saving. This kind of body can achieve high rigidity and strength, while significantly reducing weight and simplifying manufacturing processes[1-3].

Current welding methods for joining identical materials, such as steel-to-steel, can meet product design requirements. However, for the joining dissimilar materials, especially in the case of two or more layers of joining, involving TFSS and large DCAA parts, there is currently no mature and reliable joining method available[4-6]. Therefore, there is a need to develop more effective joining methods, such as FSPR. FSPR joining technology can solve the welding problem of TFSS and large DCAA parts with two-layer or three-layer plates, and realize the welding of complex BIW structures.

The selection of FSPR joining parameters is challenging because it is closely related to the plastic deformation of materials, the dimensions of convex and concave dies, feeding amount, and pressure. Therefore, establishing a rational mathematical model that provides the relationship between the die dimensions, feeding amount, and arc-gap dimensions is

Received 2024-03-06.

* Corresponding author: Lijun Han, doctor of Engineering, co-professor of Jilin University, expert of FAW-Volkswagen. E-mail: lijun.han@faw-vw.com.

significant. A rational physical and mathematical model can show the direct relationship between parameters such as the die feeding amount and the arc-gap, enabling the rapid determination of joining parameters to meet the requirements of production. By selecting the die gap dimensions and feeding amounts based on the joint design requirements, a reasonable filling gap and well-formed joining can be obtained, thereby satisfying the mechanical performance requirements of the joint.

1 Materials and Methods

1.1 Experimental Materials

The experimental materials utilized in this study include body covering steel, TFSS (Tin-Free Steel), and DCAA. The compositions and mechanical properties of these materials are presented in Tables 1 to 4.

Table 1 Chemical composition of TL 4225 (wt. %)

C	Mn	Si	Al	Ti	Cr	Ni	Mo
0.22~0.25	1.20~1.40	0.20~0.30	0.20~0.50	0.02~0.05	0.11~0.20	~0.10	~0.10

Table 2 Chemical composition of C611 (wt. %)

Si	Mn	Mg	Fe	Zn	Cu	Zr	Ti	Na	Ca	Sr	Al
7.12	0.61	0.21	0.13	0.02	0.05	0.05	0.05	0.0001	0.0007	0.008	The rest

Table 3 Chemical composition of CR5 (wt. %)

C	Si	Cu	P	Mn	S	Ti	Al	Fe
≤0.02	≤0.50	≤0.20	≤0.02	≤0.30	≤0.02	≤0.30	≥0.01	The rest

Table 4 Mechanical properties of TL4225, C611 and CR5

Mechanical property	Yield strength (Mpa)	Rupture strength (Mpa)	Microhardness(HV)	Elongation(%)(A80)
TL 4225	1100	1475	400-520	≥5%
CR5	110-170	260-330	—	≥41%
C611	≤140	340	≤120	≥23%

1.2 FSPR Joining Principle

The FSPR riveting process involves feeding rivets into a rivet gun through a rivet-feeding system. During the riveting process, the rivet shears and expels the connected plates, and the surrounding area of the rivet is compressed by a concave die to achieve high-quality joining of the sheets, as illustrated in Fig.1.

To employ FSPR joining technology, the following key conditions must be met: first, the thickness of the bottommost layer should be at least 1/3 of the total thickness of the plate combination. Second, a high-hardness material should be on the side of the punch, whereas low-hardness material should be on the side of the concave die. Moreover, thin sheets should be on the punch side, and thick sheet should be on side of the concave die. The maximum strength of the upper layer is 1500 MPa. A harder upper layer can effectively support a lower layer with lower strength requirements, which can also ensure a better plasticity of the lower layer. It is essential to note that the maximum strength of the lower layer plate should not exceed the strength threshold of 600 MPa.

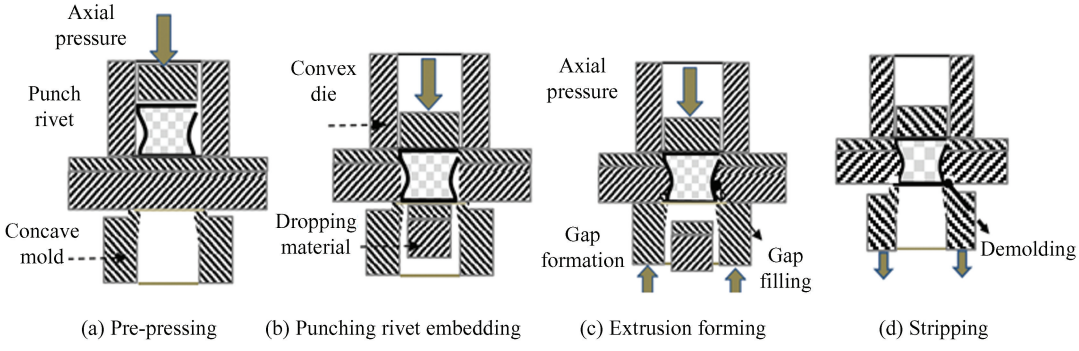

Fig.1 Principle of FSPR joining

The FSPR allows for multi-layer riveting of mixed DCAA and TFSS, with a maximum total thickness up to 9.0 mm. This yields good forming results and can be applied to coverings, such as doors. Furthermore, in terms of joint strength, the shear strength of the joints is high, which can ensure stable riveting appearance.

Based on the above description, the joining mechanism of the FSDR may be explained by the plastic flow of metals during joining. Under the extrusion action of the lower die boss, the bottom plate adjacent to the rivet attachment underwent plastic deformation and flowed. On the convex side, the width of the metal is relatively narrow; under the same conditions of yield strength, the force required for deformation is relatively low, therefore, deformation must occur on the convex side. Under convex pressure, the rheological metal flows into the curved rivet gap, resulting in a continuous increase in gap height continues. This process is essential for completing the metal rheological forming, finally achieving a strong joint formation.

2 Establishing of Mathematical Model

2.1 Joint Forming Characteristics

Fig.2 illustrates the forming characteristics of the joint surface. By controlling the dimensions of the bottom die and the Z-axis feeding value, plastic deformation occurred in the bottom soft plate, allowing the flowing metal to fill the arc-gap and achieve joint formation and plate joining. The upper surface of the joint is flush with the base material, whereas the lower surface exhibits a groove that forms because of the flow of metal, as shown in Figs.1 (a) and (c).

As a new joining method, FSPR is currently in the stage of accumulating laboratory data and partial application in car bodies. It serves as a new solution for steel/Al structure bodies.

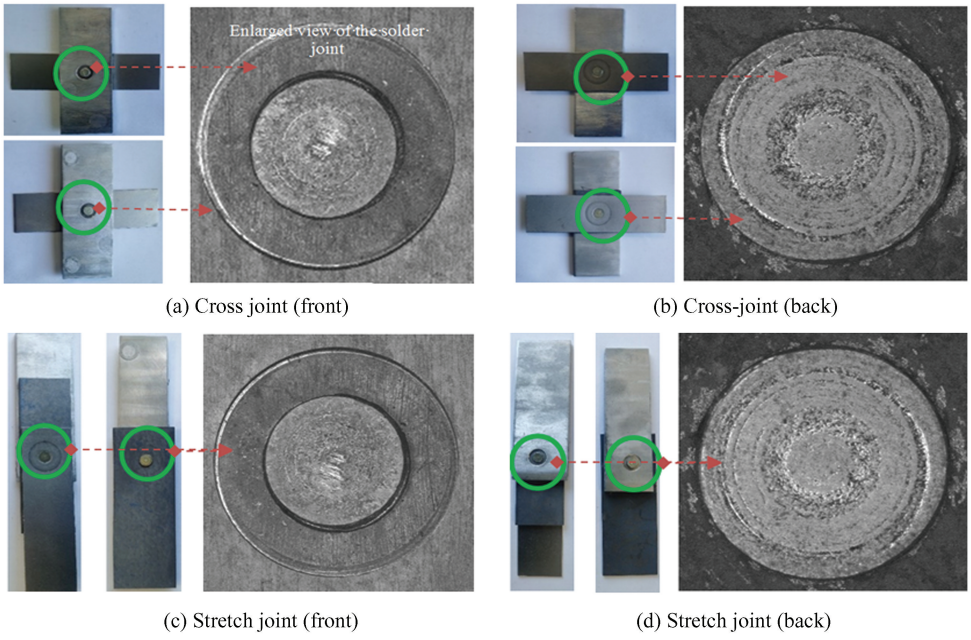

(a) Cross joint (front) (b) Cross-joint (back)

(c) Stretch joint (front) (d) Stretch joint (back)

Fig.2 Joints of FSPR

Fig. 2 presents the forming morphology of the two-layer and three-layer FSPR joints. The joint morphology varies on both sides of the joint depending on the shape of the convex die, deformation state, and forming depth.

The Experiments involved the two-layer joining of TFSS with DCAA and the three-layer joining of DCAA, TFSS, and a covering steel plate. This is the most common combination of DCAA plates in BIW with different requirements for strength and surface forming.

The key joining parameters are listed in Table 5, which include blanking pressure, forming pressure and corresponding time, and the parameters are preset. Other key parameters, such as the width of the die boss and the feed height are related to the total

thickness of the connecting plate and the length and curvature of the rivets, which is the focus of this study.

2.2 Model of Joining

The FSPR joining model for the two- and three-layer configurations is shown in Figs.3 (a) and (b). Through the action of the forming die, the matrix metal on the die side of the rivet undergoes localized plastic deformation, allowing it to be squeezed into the arc zone of the rivet, which effectively achieves a riveting effect. The effect of riveting differs for two- and three-layer plates, depending on the flow state of the metal and elastoplastic deformation during forming.

Table 5 Main joining parameters of the joint

Pre-pressure time (s)	Drop pressure (kN)	Dropping time (s)	Forming pressure (kN)	Holding time (s)
1.5	7	1.0	6	1.0

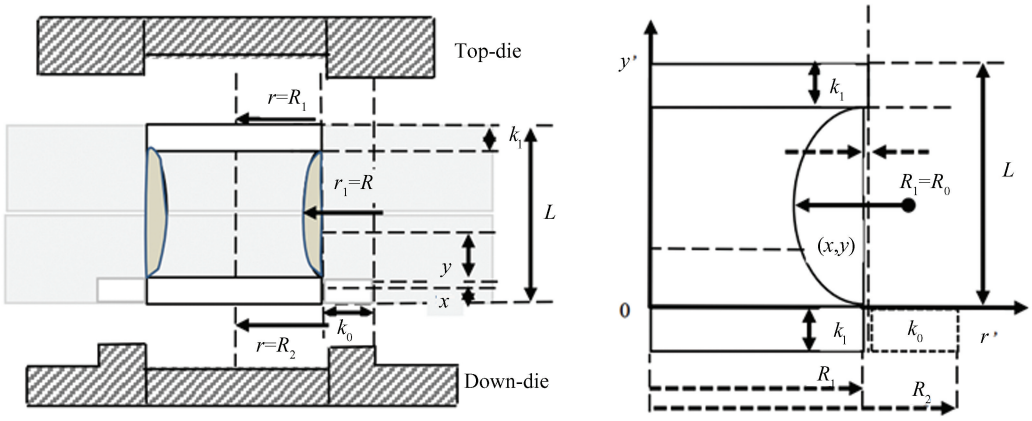

(a) Diagram of the joint and die (b) Coordinate system of FSPR model

Fig.3 Joint model of FSPR joining

For TFSS with higher hardness and yield strength, less deformation occurs, and the filling gap in the corresponding area is supplemented by the deformation of low-strength materials such as thin plates and DCAA. For the two-layer plates, the flow deformation was more substantial, and the gap filling around the rivet was more complete. The direction of metal flow and the characteristic distribution of grains along the arc during deformation are evident. In contrast, for the three layers, owing to increased thickness and gap size, as well as the elastic effect of plate materials, the plastic deformation area of the DCAA is smaller, resulting in less deformation and insufficient gap filling.

For the FSPR joining of DCAA and TFS, the joints can exhibit high tensile and shear strength, which meets the performance requirements of the product. The design of the die punch shape and dimensions directly determine the shape and size of the arc-gap filling during extrusion forming, thereby affecting the mechanical performance of the joint. Numerous factors influence the filling of the joint arc-gap, including the dimensions and shape of the extrusion die, extrusion depth, dimensions of the rivet, and the plasticity of the plate metal.

To simplify the selection of joining parameters, it is crucial to establish a scientific mathematical model for joint extrusion forming. This allows for the rapid selection of joining parameters without relying on many tested samples to obtain the proper parameters. A simplified physical model of the joint and its surrounding area is shown in Fig.3 (a), based on the physical parameters of the FSPR die, joint, and forming process. A mathematical coordinate system was introduced to establish a rational mathematical model, as shown in Fig.3 (b).

To facilitate modelling and simplify the calculations, the following definitions were made.

k_0: Width of shape-forming lug boss, R_2-R_1

k: Rivet edge height

k_1: Height of rivet top round table

R_2: Outer diameter of indentation

R_1: Inner diameter of indentation

R_0: Radius of rivet central position

r: Radius of rivet arc

r_1: Rivet arc-filled area radius

L: Rivet length

In addition, defining the depth of indentation as x and the coordinates of any point on the arc as (r, y), there is a metal volume in the extruded region:

$$v_1 = \pi \times (R_2^2 - R_1^2)x \tag{1}$$

where $0 < x < k_1$ and x is the indentation depth.

The height of the arc-gap is $L-2k_1$.

If the coordinate of any point on the arc is (r, y), the gap volume is as following in Eq.(2).

$$v_2 = \int_0^y \pi R_1^2 \, dy - \int_0^y \pi r^2 \, dy \tag{2}$$

where y denotes the height of the filling metal.

The expression for the arc is

$$(r-a)^2 + (y-b)^2 = R_0^2$$

Then, there is:

$$r = \sqrt{R_0^2 - (y-b)^2} + a$$

where:

$$a = R_1 + \sqrt{R_0^2 - (L/2 - k_1)^2}$$
$$b = L/2 - k_1$$

Therefore, there is:

$$\int_0^y \pi r^2 \, dy = \pi \int_0^y \left[R_0^2 - (y-b)^2 + a^2 + 2a\sqrt{R_0^2 - (y-b)^2} \right] dy = \pi(R_0^2 + a^2)\, y - \pi \int_0^y (y-b)^2 \, dy + 2\pi a \int_0^y \sqrt{R_0^2 + (y-b)^2}$$

$$\int_0^y (y-b)^2 \, dy = \frac{(y-b)^3}{3}\Big|_0^y = \frac{(y-b)^3}{3} + \frac{b^3}{3}$$

$$\int_0^y \sqrt{R_0^2 - (y-b)^2} \, dy = \int_{-b}^{y-b} \sqrt{R_0^2 - y^2} \, dy = \frac{y}{2}\sqrt{R_0^2 - y^2}\Big|_{-b}^{y-b} + \frac{R_0^2}{2}\arcsin\frac{y}{R_0}\Big|_{-b}^{y-b} = \frac{y-b}{2}\sqrt{R_0^2 - (y-b)^2} + \frac{R_0^2}{2}\arcsin\frac{y-b}{R_0} + \frac{R_0^2}{2}\arcsin\frac{b}{R_0} + \frac{b}{2}\sqrt{R_0^2 - y^2}$$

Thus obtained as follows

$$\int_0^y \pi r^2 \, dy = \pi(R_0^2 + a^2)\, y - \frac{(y-b)^3}{3} + \frac{\pi b^3}{3} + 2\pi a \left[\frac{y-b}{2}\sqrt{R_0^2 - (y-b)^2} + \frac{R_0^2}{2}\arcsin\frac{y-b}{R_0} + \frac{R_0^2}{2}\arcsin\frac{b}{R_0} + \frac{b}{2}\sqrt{R_0^2 - y^2} \right]$$

Based on $V_1 = V_2$, the following relationship can be obtained

$$\pi(R_2^2 - R_1^2)x = \pi R_1^2 y + \pi(R_0^2 + a^2)y + \frac{\pi(y-b)^3}{3} + \frac{\pi b^3}{3} - 2\pi a \left[\frac{y-b}{2}\sqrt{R_0^2 - (y-b)^2} + \frac{R_0^2}{2}\arcsin\frac{y-b}{R_0} + \frac{R_0^2}{2}\arcsin\frac{b}{R_0} + \frac{b}{2}\sqrt{R_0^2 - y^2} \right] \tag{3}$$

In summary, the equations for x and y are as follows:

$$(R_2^2 - R_1^2)x = (R_1^2 - R_0^2 - a^2)y + \frac{(y-b)^3 + b^3}{3} - 2a \left[\frac{y-b}{2}\sqrt{R_0^2 - (y-b)^2} + \frac{R_0^2}{2}\arcsin\frac{y-b}{R_0} + \frac{R_0^2}{2}\arcsin\frac{b}{R_0} + \frac{b}{2}\sqrt{R_0^2 - y^2} \right] \tag{4}$$

Where:

$$a = R_1 + \sqrt{R_0^2 - (L/2 - k_1)^2}$$
$$b = L/2 - k_1$$

In this test, making $R_0 = 3.6$ mm, $k_1 = 0.8$ mm, $R_1 = 3.15$ mm, $R_2 = 5.18$ mm, and $L = 5.6$ mm. Substituting the values into the formula above, we obtain the following:

$a = 6.14$ mm, $b = 2$ mm.

Eq. (4) can be rewritten as

$$(R_2^2 - 9.92)x = -40.74y + \frac{(y-b)^3}{3} - 39 - 6.14(y-2)\sqrt{13 - (y-2)^2} - 80\arcsin\cdot\frac{y-2}{3.6} - 12.28\sqrt{13 - y^2} \tag{5}$$

Under the conditions that $R_2 = 5.7$ mm, 5.5 mm, 5.18 mm, 5.0 mm, 4.8 mm and 4.5 mm respectively, the relationship between the filling height y of the arc-gap and the extrusion depth x of the die is shown in Figs.4(a~f), respectively. In Fig.4, δ represents the height compensation. This model reflects the relationship between the key parameters, including the arc-gap radius, plate thickness, radius and height of the rivet head, groove width, and feeding amount. By keeping the other parameters constant, the model can establish mathematical relationships between any two parameters, which offers a theoretical basis for the application of FSPR joining, die design, and the selection of process parameters.

2.3 Modification of the Model

The model can essentially depict the relationship between the filling height and feeding amount for two-layer plates. For the three-layer plates, as the TFSS is positioned in the middle, some elastoplastic deformation occurs near the edge of the joint under a larger punch, influencing the plastic deformation of

the flowing metal on the DCAA side and arc-gap filling. The mathematical model was modified based on the experiment, and two of the morphologies of the FSPR joints are shown in Fig.5.

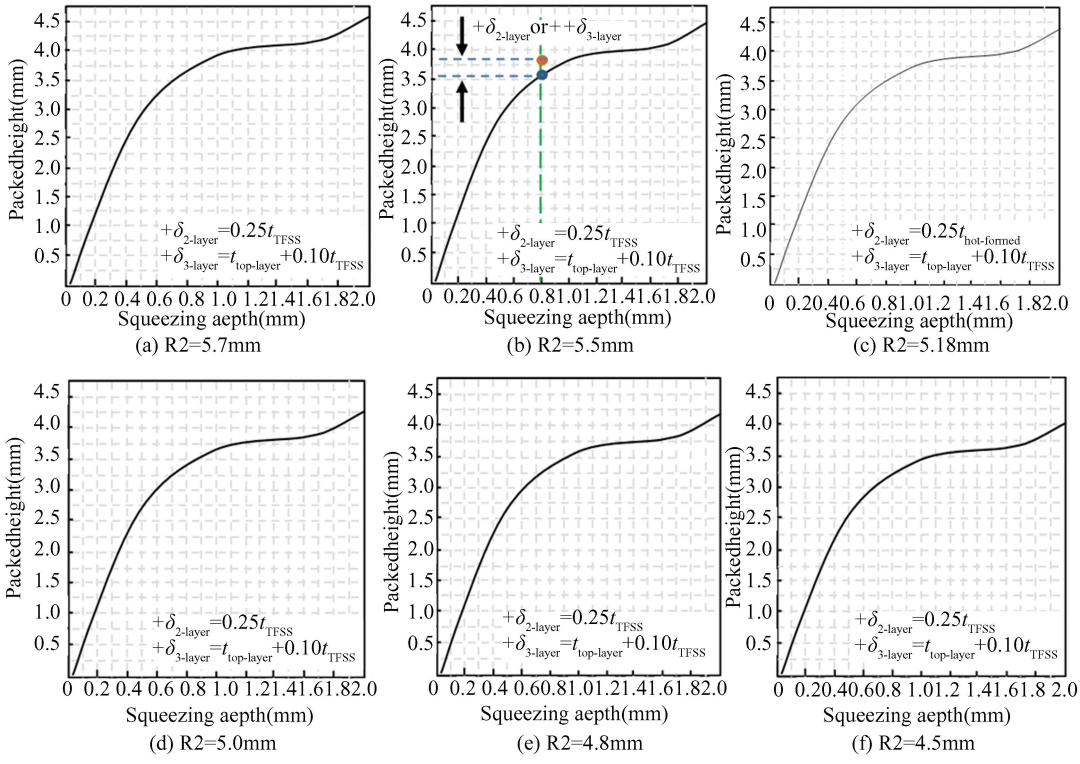

Fig.4 Relationship between extrusion depth and arc gap filling height under different extrusion radius

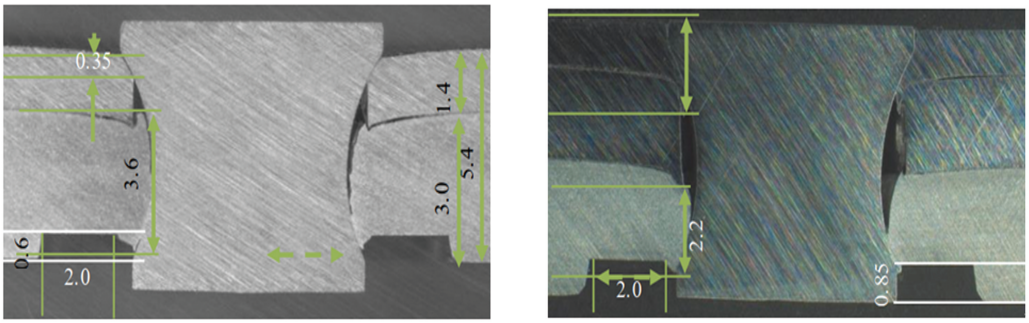

(a) Joint of two-layer plate (b)Joint of three-layer plate

Fig.5 Joint metallography

For two-layer plates, the measured feeding amount and arc-gap filling height are shown in Fig.5 (a). The height of the filled gap obtained from theoretical calculations closely matched the experimental value. The arc-gap at the TFSS end was achieved through plastic deformation during forming, with a deformation of approximately 25% of the TFSS based on experimental data. Therefore, for joining the DCAA and TFSS two-layer plates, the relationship between y and x in Eq.(5) should be adjusted by adding approximately 25%, that is to increase the thickness of the TFSS plate by $0.25t_{\text{TFSS}}$.

$$\delta_1 = 0.25\ t_{\text{TFSS}}$$

The total filling height is

$$y_{\text{total}} = y + 0.25t_{\text{TFSS}}$$

To join the three-layer plates, the plastic deformation of the top-layer plate played a crucial role in filling the arc-gap. Through its deformation, the gap within the thickness of the top layer was filled, meeting the height requirement of the top layer.

In addition, the plastic deformation of the top-layer plate was extruded into the gap within the

middle TFSS plate. Considering the total thickness of the joint and the top-layer, the filling height is approximately $0.15t_{\text{TFSS}}$. For joining with three-layer plates, the contribution of the three-layer plates to the height of the arc-gap is

$$\delta_3 = t_{\text{top-layer}} + 0.10t_{\text{TFSS}}$$

$$y_{\text{total}} = y + t_{\text{top-layer}} + 0.10t_{\text{TFSS}}$$

Experimental verification was conducted for two-layer plates, the actual gap filling height was approximately 3.95 mm, while the theoretical calculation value was 3.85 mm, as shown in Fig.4 (b). The deviation between theoretical calculations and the actual filling was within 5%. The model requires modification using mass-production data.

For three-layer plates, due to the complexity of joint deformation and the special material properties of TFSS, the filling height is influenced by multiple factors, such as the elastoplastic transformation of the TFSS joint edge zone during forming and the effect of upper layer and lower layer plates extruding into the arc-gap. If the other parameters are kept constant, the filling height of the arc-gap is approximately 3.4 mm. Whereas, the theoretically calculated height, compared to two-layer plates with the same thickness, is approximately 4.2 mm. The deviation between the theoretical calculation and the actual joint values was approximately 20%. Therefore, plate thickness has a significant impact on the calculation, and the two-layer plate model cannot simply replace the three-layer plate model. It is necessary to recalculate the values of a and b, and use them in Eq. (4) for further calculations. More production and test data are required to make necessary modifications to the mathematical model for other combinations of plate thickness, aiming to achieve calculations closer to actual data.

2.4 Joint Performance Test

Based on the above parameters and conditions, the tensile and shear strengths of the two-and three-layer plate joints, shown in Fig.5, were tested, and the results are shown in Figs.6~9.

These curves illustrate the strength relationship between the TFSS and the DCAA under the same joining parameters and plate thickness shown in Figs.6~9, including two- and three-layer plates. It can be observed from Figs.6~9 that both the tensile strength and yield strength are significantly influenced by the filling height of the arc-gap, with a notable difference.

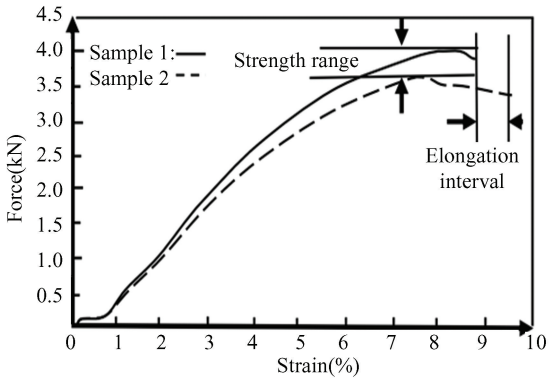

Fig.6 Tensile strength curve of the 2-layer plate joints

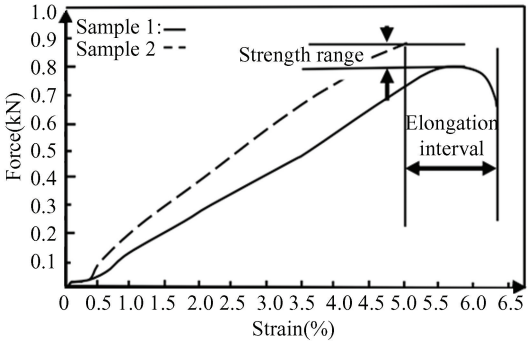

Fig.7 Tear strength curve of the 2-layer plate joints

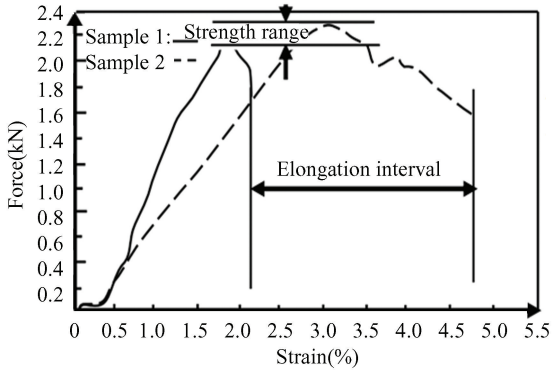

Fig.8 Tensile strength curve of the 3-layer plate joints

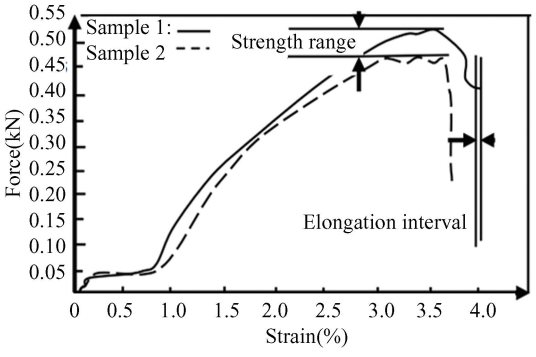

Fig.9 Tear strength curve of the 3-layer plate joints

3 Conclusions

(1) This study investigated the principles of

FSPR joining technology, joint forming mechanism, forming characteristics, and influencing factors of the joint surfaces. During the riveting process, the filling height in the arc-gap significantly affects the joint strength. Analysing the relationship between arc-gap height, die dimensions, and extrusion depth is particularly important, which can simplify the testing for choosing the process parameters, reduce time, and improve accuracy.

(2) Based on the forming characteristics of the FSPR joining technology, the characteristics of plate thickness combinations, rivet dimensions, die dimensions, and extrusion depth, a mathematical model was established to simulate the relationship between the joint arc-gap filling height and parameters, such as die extrusion depth and extrusion groove size. By maintaining a consistent set of conditions, the model allows for a clearer simulation on how variations in the filling height directly affect the extrusion depth. Similarly, by fixing the extrusion depth, the relationship between the arc filling height and extrusion groove width can be explored.

(3) Considering the characteristics of joint formation for two- and three-layer plates, a mathematical model was established to compensate the filling height of the arc-gap in the extrusion of flowing metal in DCAA. The compensation of the filling height for the two-layer plate mathematical model was 25% of the TFSS thickness. For the three-layer plates, the compensation value was the thickness of the top thin plate plus 15% of the TFSS thickness. This model can accurately predict the filling height of the arc-gap for two-layer plates, however, further optimization and verification are needed for three-layer plates.

References

[1] Han L, Yu L, Zhang G, et al. Principles and application of RES welding technology. China Welding, 2019, 28(2): 50-55. DOI: 10.12073/j.cw.20190128001.

[2] Meschut G, Janzen V, Olfermann T. Innovative and highly productive joining technologies for multi-material lightweight car body structures. Journal of Materials Engineering and Performance, 2014, 23(5): 1515-1523. DOI: 10.1007/s11665-014-0962-3.

[3] Hoerhold R, Müller M, Merklein M, et al. Mechanical properties of an innovative shear-clinching technology for ultra-high-strength steel and aluminium in lightweight car body structures. Welding in the World, 2016, 60(3): 613-620. DOI: 10.1007/s40194-016-0313-0.

[4] Zhao H, Han L, Liu Y, et al. Analysis of joint formation mechanisms for self-piercing riveting (SPR) process with varying joining parameters. Journal of Manufacturing Processes, 2022, 73(6): 668-685. DOI: 10.1016/j.jmapro.2021.11.038.

[5] Meschut G, Hein D, Gerkens M. Numerical simulation of high-speed joining of sheet metal structures. Procedia Manufacturing, 2019, 29: 280-287. DOI: 10.1016/j.promfg.2019.02.173.

[6] Park N, Kim S, Kim N. Self-piercing rivet joining of multi-material including CFRP: Experiments and FE modeling. Composite Structures, 2023, 321: 117341. DOI: 10.1016/ j. compstruct.2023.117341.

[7] Li F, Sui X, Xu P, et al. Effects of process conditions on the matched cold-pressing joining quality between dissimilar sheets. The International Journal of Advanced Manufacturing Technology, 2015, 76: 1837-1843. DOI: 10.1007/s00170-014-6414-2.

[8] Karathanasopoulos N, Pandya K S, Mohr D. An experimental and numerical investigation of the role of rivet and die design on the self-piercing riveting joint characteristics of Al and steel sheets. Journal of Manufacturing Processes, 2021, 69(1): 290-302. DOI: 10.1016/j.jmapro.2021.07.049.

[9] Hiroyuki K, Kaizu K, Kawamura R, et al. J0403-2-5 Joining of cold-reduced carbon steel sheets by self-punching riveting. The Proceedings of the JSME Annual Meeting. Tokyo: JSME, 2010, 6: 367-368. DOI: 10.1299/ jsmemecjo. 2010.6.0 _367.

[10] Abe Y, Saito T, Mori K I, et al. Mechanical clinching with dies for control of metal flow of ultra-high-strength steel and high-strength steel sheets. Proceedings of the Institution of Mechanical Engineers Part B: Journal of Engineering Manufacture, 2018, 232(4): 644-649. DOI: 10.1177/0954405416683429.

[11] Sprovieri J. Advances in self-piercing riveting. Assembly, 2018, 61(9): 42-45. https://www. assemblymag. com/articles/94431-advances-in-self-piercing-riveting.

[12] Kim W Y, Kim D B, Park J G, et al. Design of helical self-piercing rivet for joining Al alloy and high-strength steel sheets. Transactions of the Korean Society of Mechanical Engineers A, 2014, 38(7): 735-742. DOI: 10.3795/KSME-A.2014.38.7.735.

[13] Huang Z, Zhou Z, Huang W. Mechanical behaviors of self-piercing riveting joining dissimilar sheets. Advanced Materials Research, 2010, 905(97-101): 3932-3935. DOI: 10.4028/www.scientific.net/AMR.97-101.393.

[14] Peng H, Chen C, Ren X, et al. Research on the material flow and joining performance of two-strokes flattening clinched joint. Thin-Walled Structures, 2021, 169: 108289. DOI: 10.1016/j.tws.2021.108289.

[15] Ren X, Zhou Z, Fan Z, et al. Influence of sheet thickness on mechanical behaviors of the clinched joints produced by single-point butt clinching process. The International Journal of Advanced Manufacturing Technology, 2022, 122: 1617-1627. DOI: 10.1007/s00170-022-09945-z.